Supplementary Information for

Marcasite/Pyrite Nanocomposites Confined in N,S-doped Carbon Nanoboxes for Boosted Alkali Metal Ion Storage

Jie Wang, Jinwen Qin, Minxia Jiang, Yixin Wang, Baifeng Yang,* Minhua Cao**

Key Laboratory of Cluster Science, Ministry of Education of China, Beijing Key Laboratory of Photoelectronic/Electrophotonic Conversion Materials, School of Chemistry and Chemical Engineering, Beijing Institute of Technology, Beijing 100081, P. R. China.

Experimental section

Material characterizations: The phase compositions of the as-prepared products were analyzed by powder X-ray diffraction (PXRD, Rigaku D/Max-2500, Cu Kα radiation). The morphologies of the samples were characterized by field-emission scanning electron microscopy (FE-SEM, JEOL, JSM-6700F) with element mapping, transmission electron microscopy (TEM, JEOL, JEM-2100F), and high-resolution transmission electron microscopy (HRTEM). The chemical states of the elements were tested using X-ray photoelectron spectroscopy (XPS, PerkinElmer PHI 1600 ESCA). Nitrogen adsorption/desorption curves were measured by the Brunauer-Emmett-Teller method to analyze the pore size distribution and specific surface area of the samples under N_2 physisorption at 77 K. The carbon content was measured by a CHNS/O analyzer (EA3000) and thermogravimetric analysis (TGA) using a Rigaku thermogravimetry analyzer in the air at 10 °C min^{-1} over the temperature range of 30-900 °C.

Electrochemical measurements: The electrochemical performances were evaluated using coin-type cells (CR2025) with lithium/sodium metal foil as the counter and reference electrodes. These tests were conducted on a LAND CT2001A testing system, with a voltage range of 0.01-3.0 V for lithium-ion batteries (LIBs), and 0.5-3.0 V for sodium-ion batteries (SIBs). The samples obtained above were used as active materials. For the anode preparation, the active material, conductive carbon black, and polyvinylidene difluoride (PVDF) with a mass ratio of 70:20:10 were mixed and ground in N-methyl-2-pyrrolidone (NMP). Then, the slurry was cast onto copper foil and dried at 120 °C for 12 h under vacuum. The mass loading of each as-prepared working electrode was around 1 mg cm^{-2}. The LIBs were assembled in a glovebox with 1 M $LiPF_6$ in ethylene carbonate (EC)/dimethyl carbonate (DMC)/diethyl carbonate (DEC) as an electrolyte. For the SIBs, 1 M $NaCF_3SO_3$ in diglyme was adopted as an electrolyte. And Whatman glass fiber filter paper was used as a separator. The Cyclic voltammetry (CV) was performed on a CHI-760E electrochemical workstation. Electrochemical impedance spectra (EIS) were carried out on CHI-760E at frequencies ranging from 0.01 to 100 kHz. The temperature-dependent electrochemical performance was conducted by

the climate chamber (Shenzhen Kejing Star Technology Co., Ltd., China) at the different temperatures. Galvanostatic intermittent titration technique (GITT) measurements were conducted on an Arbin battery test system by charging/discharging the cells for 1 h at a constant current density of 100 mA g^{-1} with a 2 h rest duration. For the Tafel analysis, we assembled a lithium-ion/sodium-ion three-electrode cell with the Li/Na metal counter and reference electrodes. Electrochemical measurements were conducted on a CHI-760E electrochemical workstation at a scan rate of 0.005 V s^{-1} at room temperature.

Supplementary Note 1: The Warburg region in the Nyquist plots has been used to determine the diffusion/transport rate of electrolyte ions into the electrode materials according the follow relationship:

$$D_{Li} = \frac{R^2T^2}{2A^2n^4F^4C^2\sigma^2} \quad (1)$$

$$Z' = R_D + R_L + \sigma\omega^{-1/2} \quad (2)$$

$$\omega = 2\pi f \quad (3)$$

Here, R is the gas constant, T is the absolute temperature, A is the surface area of the electrode, n is the number of electrons per molecule during oxidization, F is the Faraday constant (96500 C mol^{-1}), C is the concentration of lithium-ion, and σ is the Warburg factor which is relative with Z', f is the frequency.

Supplementary Note 2: The apparent D_{Li} is estimated based on Fick's second law with the following simplified equation:

$$D_{Li} = \frac{4}{\pi\tau}\left(\frac{m_B V_M}{M_B S}\right)^2\left(\frac{\Delta E_s}{\Delta E_\tau}\right)^2 \quad (4)$$

where τ is the pulse duration, m_B, and M_B are the active mass and molar mass of the anode material, V_M is the molar volume, and S is the active surface area of the anode. ΔE_s and ΔE_τ can be obtained from the GITT curves.

Supplementary Note 3: Randles-Sevcik equation:

$$I_p = 2.69 \times 10^5 n^{3/2} A\, C_0 D_{Na}^{1/2} v^{1/2} \quad (5)$$

Where I_p is the peak current, A is the surface area of the electrode, n is the electron transfer number per reaction, C_0 is the concentration of lithium ions in electrode, D_{Na} is the diffusion coefficient of lithium ions, and v is the scan rate of CV.

Supplementary Note 4: The reaction activation energy E_a is calculated based on Arrhenius equation:

$$i = \frac{RT}{nFR_{ct}} \tag{6}$$

$$i = A\exp(\frac{-E_a}{RT}) \tag{7}$$

where T stands for operation temperature, n is the transferred electron number, A is the pre-exponential factor, R_{ct} is the charge transfer resistance, R and F represent gas constant and Faraday constant, respectively.

Supplementary Note 5: The frequencies of the Debye peak maxima, a characteristic frequency of the conductivity relaxation, can be given by the reciprocal of the conductivity relaxation time (τ) or conductivity (σ):

$$2\pi f_{max} = \omega = (\tau)^{-1} = \sigma(e_0\varepsilon')^{-1} \tag{8}$$

where ε' (real component of permittivity) is the frequency-independent permittivity, and e_0 is the permittivity of free space (8.854×10^{-14} F cm^{-1}).

Supplementary Figures

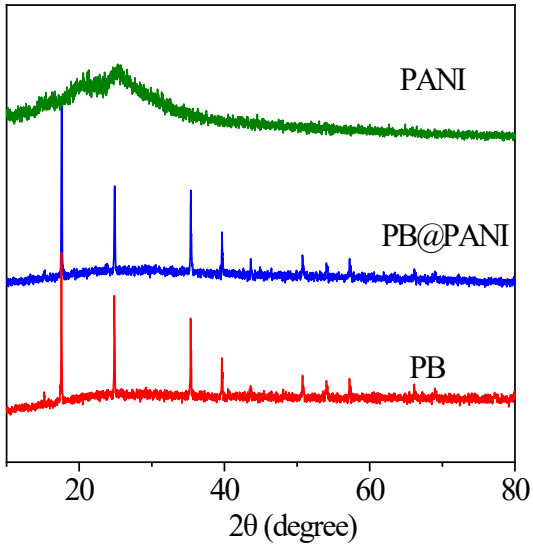

Fig. S1 XRD patterns of PB, PANI, and PB@PANI.

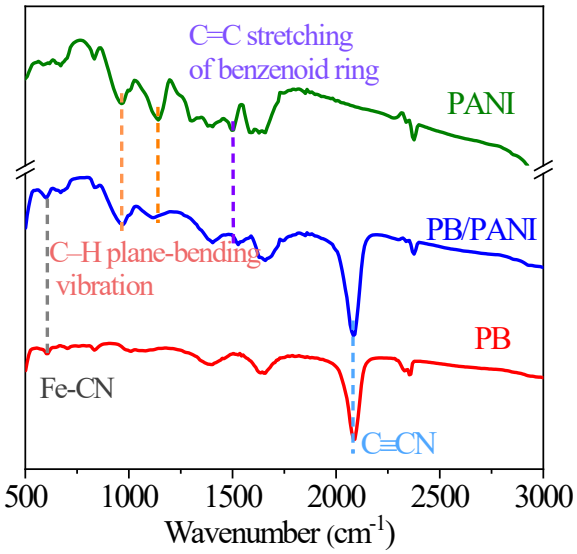

Fig. S2 FTIR spectra of PB, PANI, and PB@PANI.

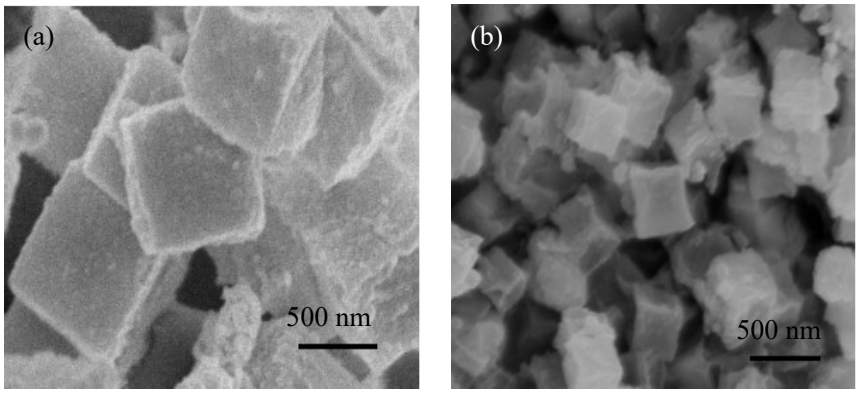

Fig. S3 (a) FE-SEM image of PB@PANI after carbonization process. (b) FE-SEM image of p-FeS_2@NSCN.

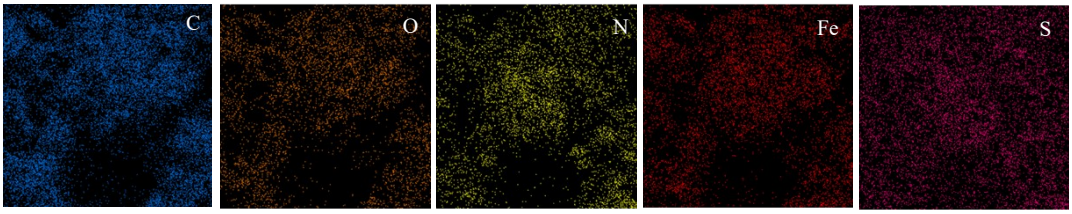

Fig. S4 Element mapping images of C, O, N, Fe, and S for m/p-FeS_2@NSCN.

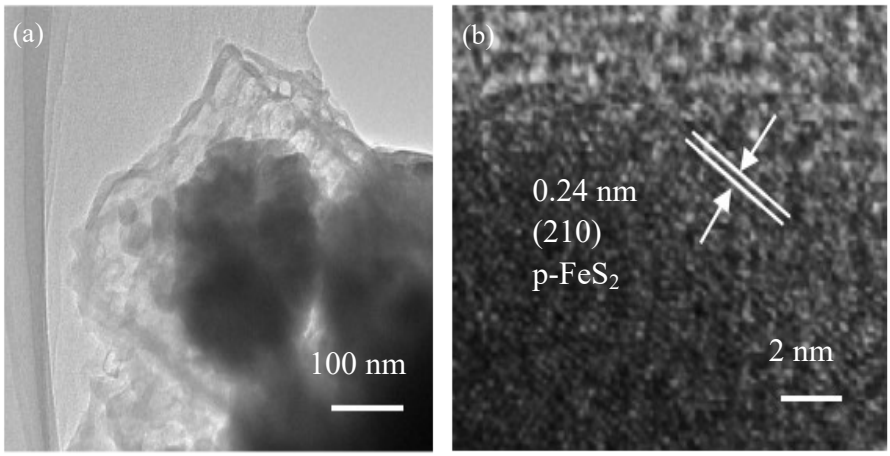

Fig. S5 (a) TEM and (b) HRTEM images of p-FeS_2@NSCN.

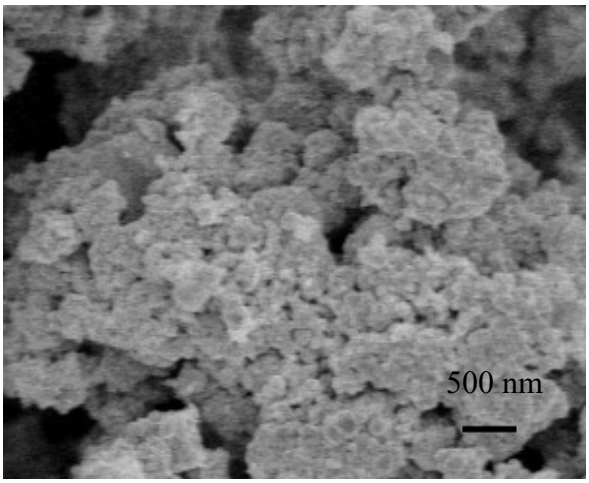

Fig. S6 FE-SEM image of p-FeS_2.

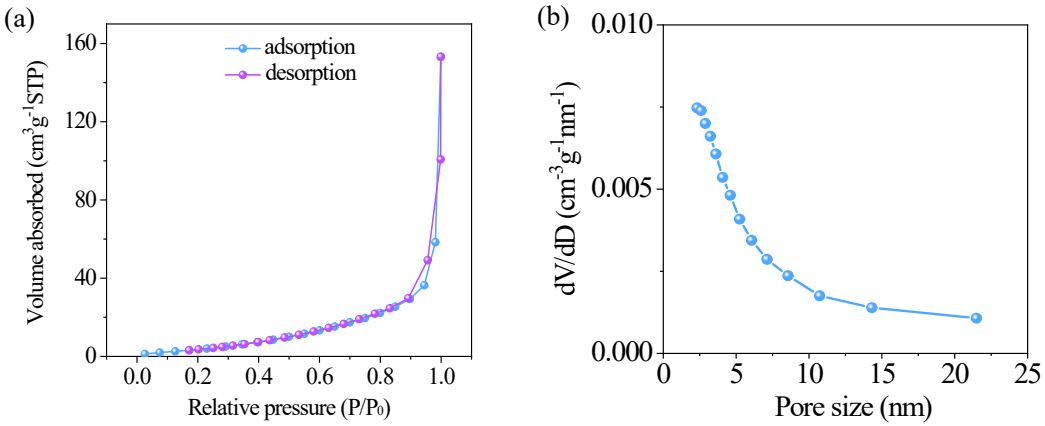

Fig. S7 (a) N_2 adsorption-desorption isotherms of p-FeS_2 and (b) its corresponding pore size distribution curve.

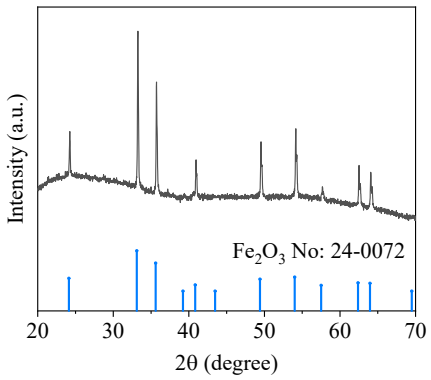

Fig. S8 XRD pattern of m/p-FeS_2@NSCN after calcination in air.

After calcination in air, m/p-FeS_2@NSCN experiences the transformation of FeS_2 to Fe_2O_3 (Fig. S8) and the oxidative decomposition of N,S-doped carbon nanoboxes. Considering that the molar amount of iron remains the same before and after the former transformation, the carbon content is calculated to be 22.5 wt%. As for p-FeS_2@NSCN and p-FeS_2, the carbon contents are determined to be 25.9 wt% and 7.5 wt%.

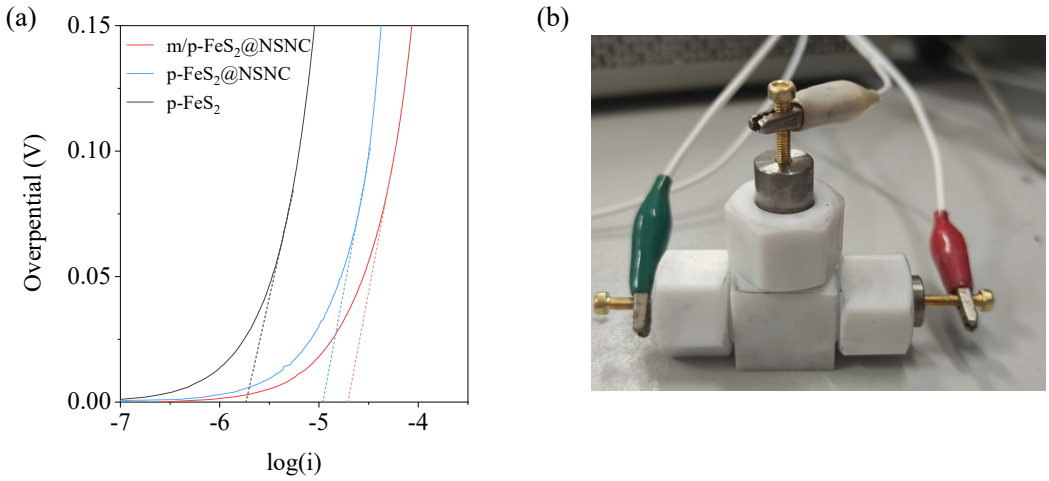

Fig. S9 (a)Tafel plot of m/p-FeS_2@NSCN, p-FeS_2@NSCN, and p-FeS_2. (b) Tests were performed in a three-electrode cell with the lithium foil as the reference and counter electrode

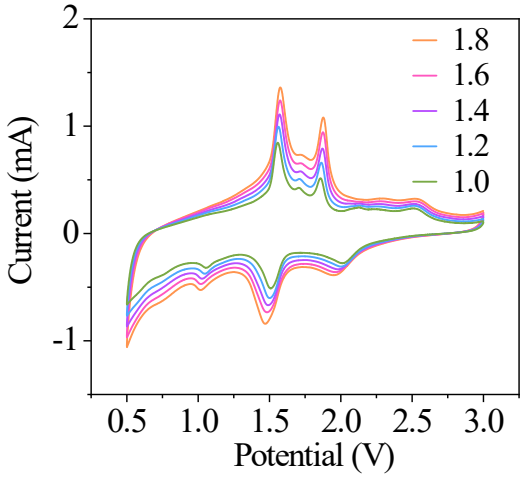

Fig. S10 CV curves of p-FeS_2@NSCN at different scan rates.

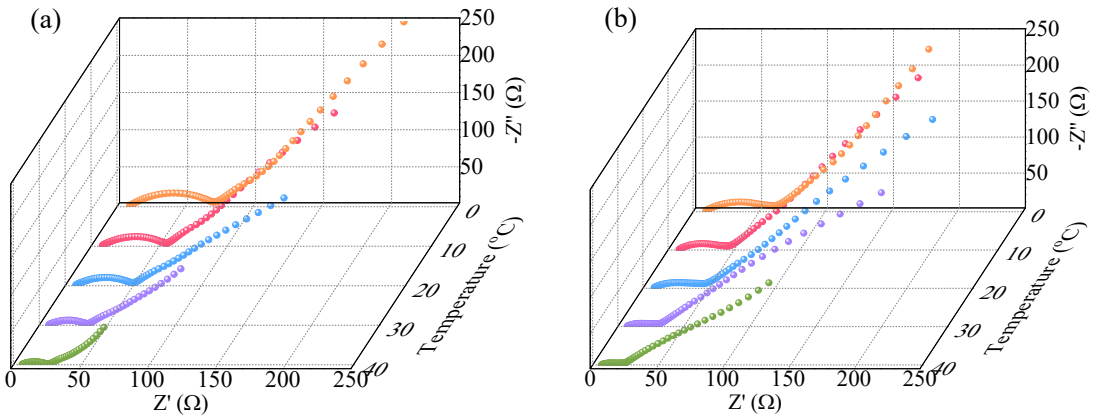

Fig. S11 Temperature-dependent EIS of p-FeS_2 and p-FeS_2@NSCN electrodes.

Table S1 The carbon contents of m/p-FeS_2@NSCN, p-FeS_2@NSCN, and p-FeS_2.

Sample / Test method	m/p-FeS_2@NSCN	p-FeS_2@NSCN	p-FeS_2
TGA	22.5wt%	25.9wt%	7.5%
CHNS/O analysis	20.1wt%	24.7wt%	6.8%

Table S2 Deconvolution results for XPS spectra of m/p-FeS_2@NSCN.

XPS spectra	**Assignment**	**Position (eV)**	**Area (cps eV)**
Fe 2p	Fe^{2+} $2p_{3/2}$	706.9	1495.2
	$Fe^{3+}2p_{3/2}$	710.9	2016.5
	satellite peak $2p_{3/2}$	714.3	490.4
	Fe^{2+} $2p_{1/2}$	719.8	653
	$Fe^{3+}2p_{1/2}$	723.8	904.1
	satellite peak $2p_{1/2}$	726.9	240.4
S 2p	S2- 2 $2p_{3/2}$	162.3	1900
	C-S-C $2p_{3/2}$	163.5	998.7
	Sulfate $2p_{3/2}$	164.3	701.2
	S2- 2 $2p_{1/2}$	165.5	350
	C-S-C $2p_{1/2}$	168.8	800.1
	Sulfate $2p_{1/2}$	169	390.7
C 1s	C=C/C-C	284.6	4232.8
	C-S	285.2	2082.5
	C-N	285.8	1382.5
	C-O	286.4	1050.9
	C=O	287.6	898.4
	O-C=O	288.6	535.8
N 1s	pyridinic-N	398.5	6086.1
	pyridinic-N	400.3	1900.4
	graphitic-N	401.6	1203.4

Table S3 The values of R_{ct} and R_{SEI} of m/p-FeS_2@NSCN, p-FeS_2@NSCN and p-FeS_2 after 100 cycles.

Sample	R_{SEI} (Ω)	R_{ct} (Ω)
m/p-FeS_2@NSCN	50.5	59.4
p-FeS_2@NSCN	54.7	84.8
p-FeS_2	74	173.9